Received: Added at production | Revised: Added at production | Accepted: Added at production

DOI: xxx/xxxx

RESEARCH ARTICLE

Optimization under uncertainty for robust fuel cycle analyses

A. V. Skarbeli*[1,2] | F. Álvarez-Velarde[1] | V. Bécares[1]

[1]Department of Energy, CIEMAT, Madrid, Spain
[2]Department of Energy Engineering, Universidad Politécnica de Madrid, Madrid, Spain

Correspondence
*CIEMAT, Av. Complutense 40, 28040 Madrid, Spain. Email: a.villacorta@ciemat.es

Summary

Optimization of nuclear fuel cycles is essential for experts and policy makers for studying and analyzing the future of the nuclear energy. In the case of advanced electronuclear transition scenarios, multiple parameters with a complex dependence have to be fine-tuned in order to achieve a set of predefined objectives. However, in the presence of uncertainties the solutions obtained in this way may not be stable since small perturbations could break the delicate balance between different parts of the scenario. In this work, the ~~robustness against uncertainties of an optimized~~ optimization of an uncertainty European-based sustainable transition scenario has been studied. This scenario, which has been analyzed with the TR_EVOL nuclear fuel cycle simulator system, ~~aims to reduce~~ is aimed at reducing the transuranic inventory masses while keeping the fuel cycle costs. To that end, an extension of the DEMO evolutionary multiobjective algorithm has been implemented within TR_EVOL for allowing the inclusion of constraints and uncertainties with a methodology that can be used by any fuel cycle simulator. Results show the importance of coupling optimization and uncertainty analyses due to the suboptimal and unstable solutions that can be obtained if not considered jointly. In addition, the uncertainties shrink the decision space. It was found that in ~~the presence of uncertainties,~~ their presence the transuranic mass can be reduced and stabilized by a factor ranging between 65%–71% with an increase of the cost of 16%–18.5% after 300 years of operation by using advanced systems when compared with an open fuel cycle strategy.

KEYWORDS:
Nuclear fuel cycle, Sustainability, Optimization, Uncertainty, Robustness

1 | INTRODUCTION

The complexity of the nuclear fuel cycle has driven the development of nuclear fuel cycle simulators. These tools have become crucial for researchers and policy makers and are extensively used for predicting and evaluating the performance, viability and sustainability of a particular electronuclear scenario in the mid and long term[1,2]. This approach implies that the desired scenario

is firstly parametrized in terms of a set of particular input parameters and then, when the simulation is completed, different metrics measuring the quality of the solutions are obtained. These metrics can include, among others, the consumption of natural uranium, the radiotoxicity of the spent nuclear fuel or the levelized cost of electricity. Nonetheless, in decision making the inverse problem is presented. The desired outcomes of the scenario are firstly defined, and given a relaxed set of initial conditions, the best case fulfilling the requirements has to be found. Taking into account the large design space that can be explored, it is clear that this is not an easy task. For ~~that~~ this reason, in the recent years nuclear fuel cycle simulators have been upgraded for performing optimization analyses in an automatized way without user interaction (see for example[3,4]).

Additionally, uncertainty analyses in fuel cycle simulations have recently gained attention ~~too~~ [5,6,7]. In general, these studies show that the uncertainties might impact on the robustness of the scenarios since perturbations ~~might~~ could break the equilibrium balance between different facilities or processes. This aspect is crucial in optimization studies since during the optimization ~~(that is,~~ process (minimization or maximization) ~~process~~ certain materials stocks (*e.g.* the Pu required to manufacture fast reactor fuel) can be pushed to the limit beyond which the scenario is no longer viable due to a lack of material, producing a broken scenario. ~~For example, consider a fast system for which one year there is not enough Pu for its fuel fabrication: its energy demand will not be satisfied due to a lack of material.~~ Therefore, if the scenario has been optimized without uncertainties (replacing for example the random variables by their expectation or reference values), there is no guarantee that when input parameters are selected from random sampling, the scenario will remain stable and/or viable.

Some studies have been conducted by the nuclear fuel cycle community ~~for accounting for the~~ to investigate effect of uncertainties in optimization problems. For example, Kunsch[8] uses a multiobjective stochastic linear programming for evaluating the best policy for the light water reactors (LWR) spent nuclear fuel (SNF). In another work, Lee[9] performs a sensitivity analysis in a case aimed to find the best growth pattern in a scenario consisting of LWR and sodium fast reactors (SFR) ~~,~~ also employing linear programming~~too~~. In Hays[10], a transition scenario from LWR to fast breeder reactors is optimized with the simulated annealing algorithm, showing also the effect of varying the uranium conversion ratio or the costs. Nevertheless, linear programming techniques assume that the objective function and constraints can be expressed in linear form. This cannot be assumed in general, as Passerini[11] shows by comparing the results of a multiobjective transition nuclear scenario solved with linear programming and a genetic algorithm. Hence, global optimization techniques should be chosen. In addition, given that changes in the input parameters have the ability to transform the results of the optimization as the mentioned works have shown, it is clear that the uncertainties must be part of the optimization problem so their effect in the objectives can be ~~captured~~assessed.

In this work, a methodology ~~to~~ for solving an optimization problem while considering the uncertainty in input parameters is discussed. In general, in multiobjective problems there is not a single optimal solution but a collection of them since improving one objective may be at the expense of worsening another. Under this consideration, a solution it is said to dominate another solution if it improves at least one objective without degrading the others. The set of all dominant solutions form the so-called

Pareto front. In order to obtain this front, the Transition Evolution code (TR_EVOL) nuclear fuel cycle simulation system [12,13] has been upgraded with an evolutionary algorithm able to solve multiobjective constrained optimization problems. The constraints, *i.e.* the conditions that have to be fulfilled, are embedded in a penalty function. In addition, in order to handle uncertainties, the expectation of the random functions are evaluated.

This methodology has been applied to an advanced European transition scenario in which Generation IV technologies are added to a LWR fleet with the objective of reaching the best sustainable scenario. A scenario is defined to be sustainable if it can be perpetuated indefinitely in time because the inventories have been stabilized. The ~~problem~~ main objective of this work is to solve, in the presence of uncertainties, an optimization problem to find a scenario minimizing the cost and stabilizing the TRU inventories according to the sustainability definition. The problem has been solved with and without uncertainties, analyzing the robustness of the solutions and comparing both results in order to show the limitations of ignoring the uncertainties during the optimization.

2 | SCENARIO DESCRIPTION

The scenario chosen for this study is based on the one investigated under the CP-ESFR project (Collaborative Project for a European Sodium Fast Reactor~~(CP-ESFR)~~ [14]. Framed in a European collaborative strategy, the scenario defined in this project considers an initial fleet of Generation II LWR that is replaced by a fleet consisting of only SFR systems with a middle phase where European Pressurized Reactors (EPR) and SFR coexist in order to produce enough Pu for feeding the SFRs. In this paper, we have redefined this scenario with the objective of pursuing both minimization of the transuranic (TRU) inventories and minimization of costs. For this reason, the SFR design has been adapted to act as a burner instead of as a breeder reactor. Furthermore, Accelerator-Driven Subcritical systems (ADS) have been introduced for burning the minor actinide (MA) inventories, in particular Am, Np and Cm. The flowchart of this new scenario is ~~shown~~ sketched in Fig. 1~~. It describes~~, showing the main facilities and stocks of materials of the cycle as well as the connections between them. As indicated in the figure, this scenario which starts in year 2010 and ends in ~~2030~~2300, contains three differentiated phases:

1. Initial phase (2010–2040): the fleet consists entirely of Pressurized Water Reactors (PWR) using either Uranium Oxide (UOX) or Mixed Oxides (MOX) fuel (denoted respectively as PWR(UOX) and PWR(MOX)). There also exists a legacy inventory of SNF which accounts for the current European legacy (see Table A1 in A). Given that this is a representation of an existing fleet, this will be the shortest phase.

2. Burning phase (2040–2100): the initial fleet gradually transitions during 20 years (2040–2060) to a new one consisting of EPR, SFR and ADS systems, with the objective of burning as much TRUs as possible. After this replacement, the

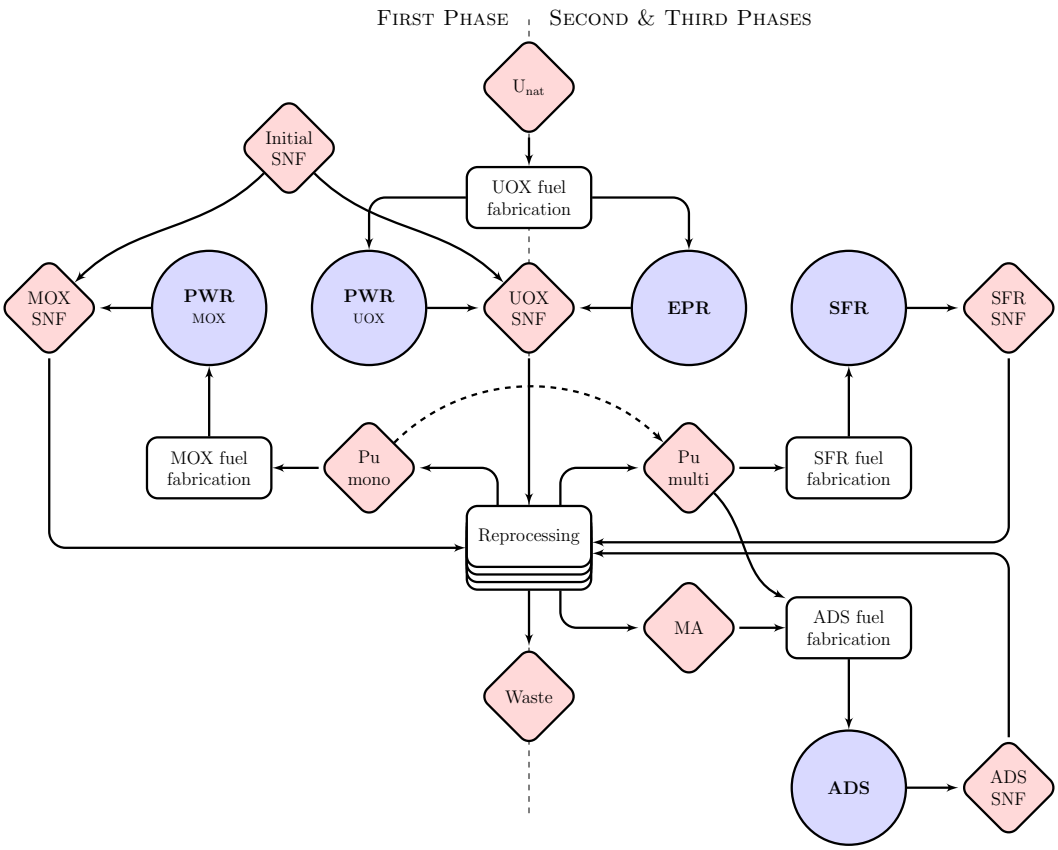

FIGURE 1 Main facilities in the scenario. The circles corresponds to the different reactor technologies, the diamonds to the stocks of materials and the boxes represents the facilities.

composition of the fleet remains stable between 2060 and 2100. The phase extends over one generation of nuclear power plants (assuming an operating life of 60 years).

3. Stabilization phase (2100–2300): starting in year 2100 the burner fleet composition is readapted in order to reach a sustainable level in which the TRU inventories do not increase nor decrease. This transition also has a duration of 20 years (from 2100 to 2120) after which no further modifications are made to the fleet. The phase will be simulated for 200 years in order to have enough time to observe the stabilization of the inventories.

During the whole scenario, the electricity production is fixed at 800 TWh_e per year as in the CP-ESFR scenario. In the first phase, 43.83 TWh_e/year are produced by the PWR(MOX) systems while the rest comes from the PWR(UOX). The ~~power~~ energy share of PWR, EPR, SFR and ADS reactors in the forthcoming phases are the free parameters which are going to be optimized in order to fulfill the scenario objectives (minimization of TRU inventories and costs). They will be precisely defined in Section 2.5. In Sections 2.1 to 2.4, the fuel cycle parameters are specified. ~~If these parameters are not explicit referenced~~When no reference for the values of the parameters is explicitly provided, they must be taken as assumptions of our study.

TABLE 1 Reactor features.

Reactor	Power (GW_e)	Thermal eff. (%)	Load factor (%)	Core mass (t_{HM})	Burn-Up (GWd/t_{HM})
PWR(UOX)	1.008	34.0	80.84	79.462	50.0
PWR(MOX)	1.008	34.0	80.84	79.067	45.0
EPR	1.652	36.0	90.00	123.513	55.0
SFR	1.440	40.0	90.00	78.120	100.0
ADS	0.154	40.0	87.00	5.325	78.3

2.1 | Reactor technologies

Main reactor parameters are shown in Table 1. In the case of the PWR(UOX), PWR(MOX) and EPR reactors, these specifications were taken from the CP-ESFR project. On the other hand, the SFR is based on the ESFR-SMART (European Sodium Fast Reactor Safety Measures Assessment and Research Tools) project design [15] while for the ADS, the EFIT (European Facility for Industrial Transmutation) concept [16] was selected. The operating life of the units has been assumed to be 60 years in all cases.

2.2 | Fuel specification

The fuel specifications can be found in Table 2. The UOX and EPR fuels are ~~made~~ produced from U_{nat}. The Pu recovered from the reprocessed UOX SNF is mixed with depleted uranium and is monorecycled in MOX fuels by the ~~PWR systems~~ PWRs until their complete decommission at the ~~ending~~ end of the first transition between the initial and the burning phase (year 2060). During the burning and stabilization phases, all the Pu and MA are multirecycled and reused as part of the SFR (using Pu and U_{dep}) and ADS (Pu, Np, Am and Cm) systems fuels. If there is not enough multirecycled Pu for these systems, the monorecycled stock will be used, as depicted with the dashed line in Fig 1. The Pu content of the SFR fuel, calculated according to the Baker&Ross equivalent method [17], has been increased compared to the original design in order to have a Pu burner reactor. This flexibility is already available in some reactors, like for instance the Japanese SFR which can be changed from low breeder to high breeder modifying its assembly design and cycle length [18]. Note that in our case, the modification will surely impact on the safety coefficients of the reactor. However, as this issue is beyond the scope of this work in the following we will assume that the reactor design remains unchanged with no safety concerns. Finally, the fabrication time is two years, and the cooling period is set to 5 years (same than CP-ESFR scenario).

2.3 | Reprocessing

Homogeneous reprocessing has been considered in this study. UOX SNF reprocessing starts with the scenario (in year 2010) while MOX SNF reprocessing starts in year 2035. Both the initial SNF legacy and the SNF produced by the ~~PWR~~ PWRs during the scenario are reprocessed in these plants. For the SFR and ADS fuels, it has been assumed that all the material is reprocessed

TABLE 2 Fuel specifications

Parameter	Value
^{235}U enrichment for UOX	4.20%
^{235}U enrichment for EPR	4.50%
^{235}U enrichment tails	0.25%
Pu content for MOX	8.65%
Pu equivalent content for SFR	16.36%
Pu/MA content for ADS	45/55%

TABLE 3 Main parameters of the reprocessing plants.

Spent Fuel	Max. amount (t_{HM})	First year
UOX	2000	2010
MOX	850	2035
SFR	∞	—
ADS	∞	—

after the 5-years cooling period. The main assumptions used for the reprocessing plants can be found in Table 3. The reprocessing losses for all fuels are set to 0.1%.

2.4 | Introducing the uncertainty

Given the unclear position the nuclear energy will play in the European electricity mix, two major assumptions of this scenario have been considered to be affected by uncertainties. ~~The first one is~~ First, that the energy production of the nuclear fleet will remain constant at 800 TWh_e ~~/~~per year during the burning and stabilization phases. Second, the maximum reprocessing capacity of the cycle ~~is~~ set at 2850 t_{HM} plus the ability of reprocessing all the SFR and ADS SNFs. The lack of knowledge ~~in the nuclear energy future~~ about the future of the nuclear energy, and thus of both assumptions, will be parametrized with an (arbitrary) variation of $\pm$10% of the values described in the previous lines in order to show the impact uncertainties have in the optimization problem.

2.5 | Defining the objective function

As stated above, the objective of this study is to obtain the optimum sustainable scenario. However, this statement must be precisely defined since the optimum scenario could be determined depending on multiple criteria. For this study, the TRU inventory masses and the fuel cycle cost at the end of scenario in year 2300 are considered. The TRU inventory masses will be measured as the total Pu and MA masses present at all the stages of the cycle depicted in Fig. 1 (fabrication and reprocessing plants, reactor cores and storage facilities). Reprocessing losses are not included in the inventories.

TABLE 4 Cost of each technology from the bibliography and fleet values considering 60 years of operating life. No EPR information was available in [20], so for this particular work, LWR costs are assumed also for EPR since according to [19] both are quite similar.

Tech.	Reference [19]			Reference [20]			Average
	Capital (€/kW$_e$)	O&M (€/(kW$_e$ y))	Fleet/Fleet$_{EPR}$	Capital ($/kW$_e$)	O&M ($/(kW$_e$ y))	Fleet/Fleet$_{EPR}$	Fleet/Fleet$_{EPR}$
EPR	3002	75	1	4300	72	1	1
SFR	3902	86	1.21	4700	78	1.09	1.15
ADS	14760	223	3.75	13900	319	3.83	3.80

Regarding the nuclear fuel cycle cost, it will be measured as the relative cost of the proposed scenario with respect to a LWR fleet in an open fuel cycle with the same installed power. In order to estimate this relative cost, only investment capital and operation & maintenance (O&M) have been considered, since in similar scenario studies they have been shown to account for 80% of the nuclear electricity costs [19]. Thus, as a first approximation fuel and decommission, dismantling & disposal costs will not be considered in this study. Table 4 outlines ~~the~~ these capital and O&M costs, obtained from [19,20]. In this way, the cost of each fleet has been estimated from the sum of the capital costs plus O&M costs during 60 years of reactor operational life. Relative costs calculated as the average of the two provided references in this way with respect to a fleet consisting only of LWRs are given in the last column of the table. ~~Finally, the~~ The figures provided for the scenario cost are obtained by integrating this relative cost from the beginning of the burning phase to the end of the scenario.

Besides, there are two implicit constraints in this scenario. The first one, related with the lack of materials during the simulation (scenario breaking), demands that ~~the TRU mass needed~~ there must always be some stock of TRUs available for new fuel fabrication ~~cannot exceed the available mass which is represented in Fig. 1 as the~~ (denoted as $Pu_{mono/multi}$ and MA stocks ~~.~~ in Fig. 1).

The second one is a consequence of the sustainability goal: the inventories have to be stabilized and thus they can neither increase nor decrease along the years. The first ~~case~~ condition can be mathematically described with an equality constraint which reflects that no additional mass should be added to the scenario in order for it to be implementable, that is $m_{add} = 0$. For the stabilization, the condition will be described with an inequality constraint demanding that the ~~change~~ variation in the TRU mass inventories must be less than certain value per year or period of time. It has been assumed, to limit the computational cost of the constraint, that this change must be less than a ton for the last ten years of the simulation. Hence, given that the simulation ends in year 2300, this constraint will be defined as $\Delta m_{TRU}(\boldsymbol{x}) := \sum_i \left| m_i(\boldsymbol{x}, t = 2300) - m_i(\boldsymbol{x}, t = 2290) \right|$ with $i \in \{\text{Pu}, \text{MA}\}$. This expression has been broken down into its components to avoid solutions in which Pu and MA change in opposite directions in

such a way their sum fulfills the condition. In this manner, the optimization problem can be mathematically expressed as

$$\min_{\boldsymbol{x}\in\mathbb{R}^d} \left(m_{\mathrm{TRU}}(\boldsymbol{x}), \mathrm{Cost}(\boldsymbol{x})\right) \quad \text{subject to} \quad \begin{cases} m_{\mathrm{add}}(\boldsymbol{x}) = 0, \\ \Delta m_{\mathrm{TRU}}(\boldsymbol{x}) < c, \end{cases} \tag{1}$$

in which $\boldsymbol{x}$ are the energy shares of each technology during the burning and stabilization phases and $c = 1$ ton the maximum variation assumed.

3 | METHODOLOGY

In order to solve the optimization problem, an evolutionary algorithm has been implemented in TR_EVOL. This kind of algorithms generates a set of candidate solutions which are iteratively updated according to a series of stochastic operators. With these operators, at each step of the iterative process a new set of candidate solutions is generated after selecting the most promising ones obtained in the previous step while rejecting the worst. In this way, the solutions move randomly through the search-space but focusing on those regions that have been ~~proven~~ found to produce the best results.

In particular, the Differential Evolution for Multiobjective Optimization (DEMO) algorithm[21] has been implemented in TR_EVOL. It is an extension of the Differential Evolution (DE) method proposed by Storn and Price[22,23] in which the selection of the best solutions is achieved with a mechanism based on Pareto ranking (a solution grouping based on their dominance) and crowding distance sorting (a measurement of the density of solutions surrounding a given point). Furthermore, the algorithm has been adapted in this work for handling constraints via the ϵ level comparison[24] in which the solutions with the lowest penalty violation are preferred. This penalty violation is measured with a function constructed from the square sum of constraints of the problem and thus for the problem defined in Eq. (1) it can be defined as

$$\phi(\boldsymbol{x}) := \max\left(0, \Delta m_{\mathrm{TRU}}(\boldsymbol{x}) - c\right)^2 + m_{\mathrm{add}}(\boldsymbol{x})^2. \tag{2}$$

~~In~~ It is worthy to remark that in general it is not possible to know in advance ~~if~~ whether there exists any feasible solution, that is, a solution that fulfills all the constraints. However, with the methodology presented in the previous lines, if it does not exist, it can be easily identified since the problem will eventually converge towards the minimum (but not zero) value of $\phi(\boldsymbol{x})$ given that the ϵ level comparison always selects the solutions with the minimum penalty.

Besides, in the presence of uncertainties, the evaluation of a set of input parameters does not produce a single value. Instead a probability density function is obtained which in general will be unknown. Notice that as the constraints have to be fulfilled for all the possible values there is not guarantee that the solution obtained without uncertainties will remain stable ~~now~~when the uncertainties are considered. In order to optimize this stochastic problem, the Sample Average Approximation (see for example[25]) will be used. It consist on minimizing the expected value of the random function by using its Monte Carlo estimate.

However, since this estimate has to be calculated for every candidate solution, to reduce the computational effort in this study only parametric variations will be employed. As in this case two variables are considered to have uncertainty, the expected value of the random functions will be approximated by

$$\mathbb{E}\left[f(\boldsymbol{x},\xi_1,\xi_2)\right] \approx \frac{1}{5}\left(f(\boldsymbol{x},\xi_1^0,\xi_2^0) + \sum_{i,j\in\{m,M\}} f(\boldsymbol{x},\xi_1^i,\xi_2^j)\right), \tag{3}$$

being $f(\boldsymbol{x})$ the objective and penalty functions to be optimized, $\boldsymbol{x}$ the set of input parameters that have to be found and $\xi_i^{0/\mathrm{m/M}}$ the stochastic variables i at the parametric variations which are reference, minimum and maximum values respectively.

4 | RESULTS

In this section the results of the optimization problem are presented. The discussion has been divided in three different parts. In a first approximation, the scenario has been optimized without considering uncertainties (Sec. 4.1). These solutions will be identified as the reference solutions, and once obtained, their robustness will be analyzed in Sec. 4.2. Finally, in Sec. 4.3 the scenario has been optimized again but introducing this time the uncertainties in the energy production and the reprocessing capacity.

It is important to note that due to the metaheuristic nature of the optimization algorithm, there is no guarantee that all the possible solutions are found. In order to overcome this issue, the problem has been solved several times and the multiple solutions have been combined. In particular, nearly a million simulations have been run for this study. Nonetheless it should be mentioned that this number strongly depends on the desired precision of the final solution.

4.1 | Reference solution without uncertainty

The results of the optimization problem (*i.e.* fuel cycle cost and TRU masses at the end of the scenario), are plotted in Figure 2. The vertical and horizontal axes are identified with the relative cost and TRU inventories masses when compared to an open fuel cycle strategy respectively. Grey points corresponds to each feasible solution obtained with the DEMO optimization algorithm while the coloured curve (the meaning of the different ~~colors~~ colours will be explained in Section 4.2) represents the Pareto front formed by the dominant solutions. An L-shaped dependence between the scenario cost and the TRU inventory masses can be observed. This has an easy explanation: in order to reduce the TRU inventory more transmutation technologies (SFRs and ADSs) have to be included in the scenario increasing thus the cost. It can also be observed that for values of TRU mass/TRU $\mathrm{mass_{EPR}}$ below ∼0.272 the cost of further reducing the TRU mass rises sharply; from the slopes of the Pareto front it can be concluded that in this region burning an extra ton is nearly 20 times more expensive. The reason for this behaviour will be explained below. Finally note that the cost axis has been normalized to the cost of an open cycle in which the initial fleet is replaced by only EPR

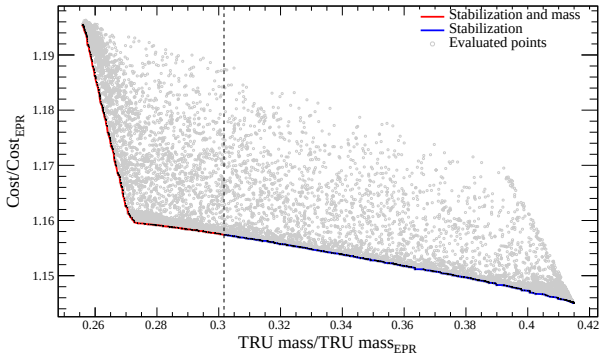

FIGURE 2 Pareto front of the optimization problem. The two ~~colors~~ colours which are separated by the vertical line, correspond to the different penalty violations of the reference case when uncertainties are considered (more details can be found in Sect. 4.2). In grey, the set of feasible (but non-dominant) solutions obtained with DEMO.

systems as explained in Sec. 2.5. For this EPR-only scenario, ~8100~~tons~~ t of TRU will be accumulated by year 300 in all stages of the scenario including the SNF legacy of Table A1. Hence, with an increase of 15%–20% in the electricity cost, the TRU stocks can be reduced by a factor that ranges between 60%–75% respectively when compared with an open fuel cycle strategy.

Pareto optimal front solutions in the input parametric space can be found in Fig. 3. This scatter matrix plot represents, for the ~~Pareto solutions~~ solutions in the Pareto front described above (in red or blue in 2), all the pairwise relationships between the two objectives (TRU and cost minimization) and the input parameters that are being optimized (energy share of each fleet by technology~~, ~~; the phase is indicated with the subscript ~~indicating the phase,~~ *e.g.* ADS_2 means ~~the~~ fraction of ADS during the burning phase and SFR_3 means the SFR fraction during the stabilization phase). Under this representation the Pareto front of Fig. 2 is placed on the Subfigure (5,1). ~~In this manner~~The interest of Fig. 3 is that, for a given point, it is possible to determine the set of input values that lead to that particular solution by projecting horizontally or vertically over the rest of the figures. For instance, the elbow previously discussed appearing when the relative cost is 1.16% and the relative TRU 0.27% (Subfig. (5,1)) is achieved when $SFR_2 = 40\%$ (Subfig. (1,1) or Subfig. (5,2)), $SFR_3 = 38.8\%$ (Subfig. (2,1)), $ADS_2 = 0\%$ (Subfig. (3,1)) and $ADS_2 = 4.8\%$ (Subfig. (4,1)).

In all subfigures, two well differentiated branches can be observed, indicating that the Pareto-optimal solutions can be ~~classified in~~ divided into two different groups for which the correlations between the inputs and the observables decompose into more simple dependencies. For this particular case, it was found that ~~it is possible to classify the solutions according to its~~ the classification can be performed according to the TRU inventory mass. This is illustrated in the figure with the different ~~colors~~colours, being each group solution defined as Orange $<$ 0.272 TRU mass/TRU mass$_{EPR}$ $<$ Blue. Looking at the Subfig. (5,1), ~~this~~ these groups can be interpreted as those solutions minimizing the TRU inventories (orange) or the cost (blue). Note that this interpretation is arbitrary in the sense that ~~there is no~~ although the groups are clearly separated, there is not technical criteria for ~~separating these solutions at TRU mass/TRU mass$_{EPR}$ = 0.272. For example, another choice would be to separate the~~

~~solutions according their penalty violation as it was performed in Fig. 2. However with the new~~ defining the solutions fulfilling TRU mass/TRU $\text{mass}_{\text{EPR}} < 0.272$ as the ones reducing the TRU inventories. Anyway, with the chosen clustering the correlations for each group are almost linear and each branch can be clearly identified (with the exception of Subfig. (4,4) in which an overlying region in the zero energy region is observed). For example, in order to maximize the reduction of TRU inventories, during the burning phase the energy share of the SFR has to be between $\sim$ 34%–42% (Subfigure (1,1)), while for the ADS this number ranges between 0%–4% (Subfig. (3,1)), existing a negative correlation between both variables (Subfig. (3,2)). On the other hand, the cheapest scenarios are obtained when no ADS are installed in the burning phase (Subfig. (5,4)) and the number of SFR is kept as low as possible (Subfig. (5,2)). Additionally, now the reason for the sharp cost increase observed below TRU mass/TRU $\text{mass}_{\text{EPR}} \sim 0.272$ ~~of TRU~~ in the Pareto front in Fig. 2 becomes clear: it is produced by the introduction of ADS during the burning phase as it is showed by the orange points in Subfig. (5,4)~~show~~.

Finally, it can be noticed that for all solutions, the ADS energy share in the stabilization phase increases when compared to the burning one: in the first case, the values are ~~lower-bounded~~ bounded by $\min \text{ADS}_3 = 4.8$ while in the latter it is verified that $\max \text{ADS}_2 = 4$ ~~. This~~ an thus $\text{ADS}_3 > \text{ADS}_2$ for all of them. Since the MA are only consumed in the ADSs this implies that the MA consumption in the stabilization phase (in which by definition inventories do not increase nor decrease) is higher than in the burning one, during which the inventories must therefore accumulate. This can be explained by a shortage in the stock of the materials used for the fabrication of the ADS fuels: as there is not enough TRU mass during the deployment of the ADS fleet (when the TRU demand is higher), the number of units that can be installed in this phase is limited by the inventories availability during this first transition. Consequently, the MA reduction of the scenario is constrained. This effect will become clearer with the discussion of the results in the forthcoming section.

4.2 | Robustness of the solutions

Once the solutions have been obtained, their robustness is studied by introducing the uncertainties in the total energy production and the reprocessing capacity. To this end, for each solution obtained in the previous section, the parametric average described in Eq. (3) is calculated and the constraint violation is analyzed as a measurement of their robustness. In this work, it was obtained that none of the solutions of the Pareto front was stable. All of them violate the stabilization constraint, while a small subset (depicted in red in Fig. 2) also required an additional mass in order to avoid scenario breaking, hence violating both constraints. The solutions that only violate the stabilization constraint are represented in blue. It should be clear that the vertical line in Fig. 2 only separates solutions located in the Pareto front. The reference non-dominant feasible solutions (*i.e.* grey points) that will violate the additional mass constraint in the presence of uncertainties could be located either to the left or to the right of this vertical line. Anyway, the red subset corresponds to the solutions minimizing the TRU inventories, since they push the stocks to the limits in order to achieve the higher TRU reduction it is understandable and expectable that they violate this mass constraint.

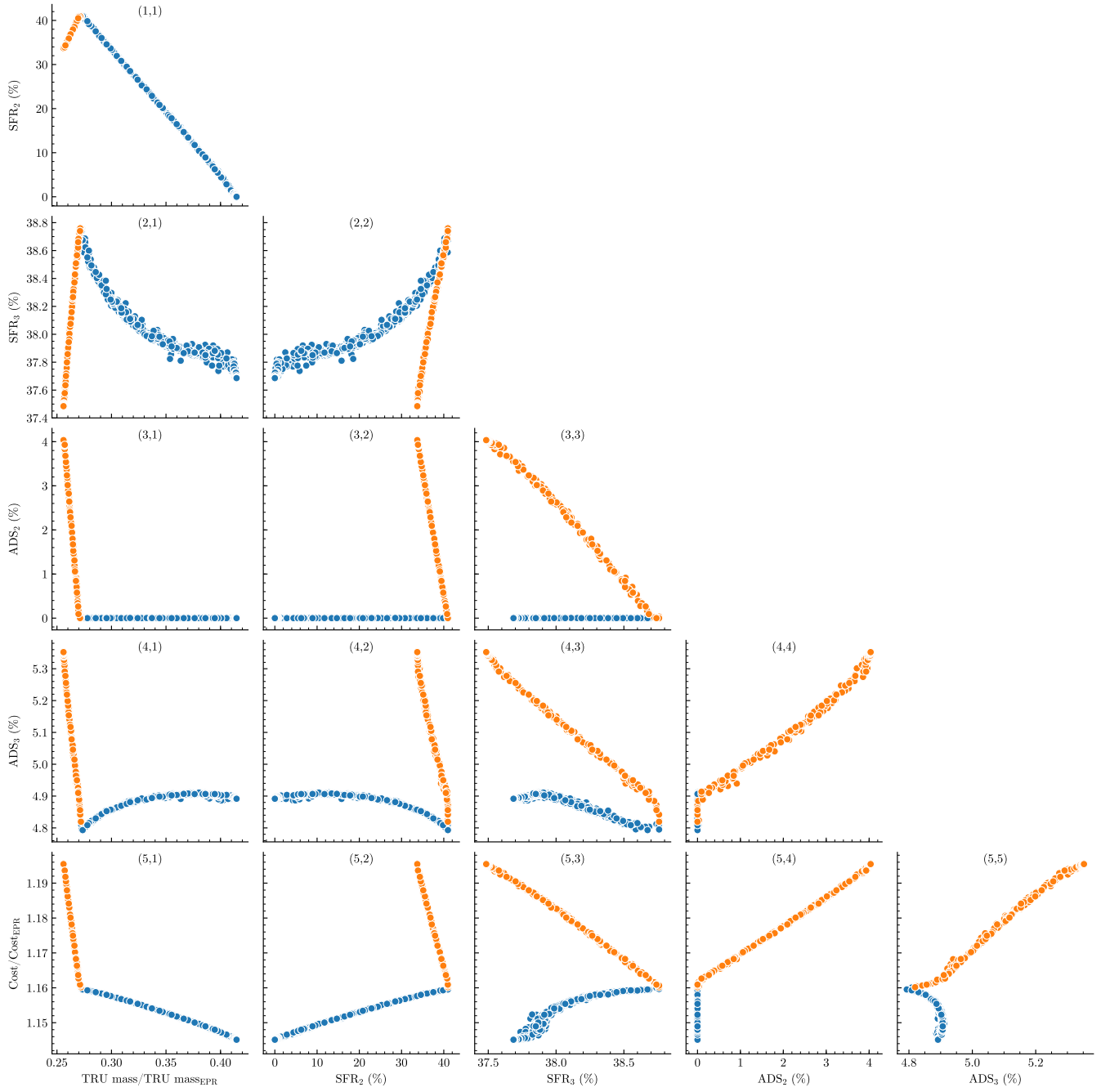

FIGURE 3 Pairwise plot of the two objectives and the input optimization parameters.The different ~~colors~~ colours group the solutions by the values of the objective functions.

This evidences the complexity of dealing with uncertainties: the process may lead to a suboptimal solution and, worse than that, there is no guarantee that this solution will be stable. Nonetheless, it should be pointed out that there exist solutions more stable than others in the sense that they only violate one of the two constraints. Therefore, if the inequality constraint were relaxed no penalty will occur for the blue solutions of the figure.

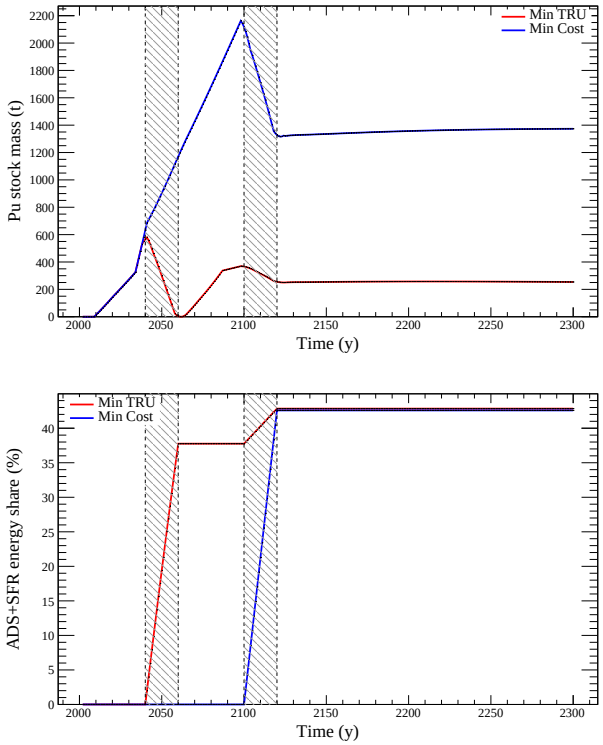

FIGURE 4 Plutonium stock (top) and burning energy share (bottom) for two of the scenarios in the Pareto front of Fig. 2. The shaded areas represents the transition between the different phases.

Fig. 4 shows an example of two unstable reference scenarios ~~of~~ located on the Pareto front. In the top figure, the Pu stock mass ~~used~~ available for fuel fabrication (see Fig. 1) is represented for one of the ~~solutions~~ scenarios minimizing the cost and that will violate the stabilization constraint when uncertainties are considered (blue line, corresponding to one of the solutions in the blue region of Fig. 2), and another solution that minimizes the TRU inventories (red line) and that will violate both the stabilization and the need of additional mass. The bottom figure shows the energy share of the burning technologies (ADS and SFR) for the same cases.

In the red scenario, the Pu stocks begins to accumulate when the UOX reprocessing plant starts its operation in year 2010, and then the slope increases when the MOX plant starts in 2035. All the initial SNF UOX and MOX inventories are completely reprocessed by years ∼2040 and 2085 respectively, which explains the ~~change~~ changes in the trend observed in the curve: as less material is recovered, for the same TRU consumption the ~~Pu stock decreases~~rate of increase of the Pu stock is reduced. In addition, during the two transitions between phases, the Pu stock is reduced due to the large consumption the deployment of new reactors (the new cores need to be fabricated and since the number of units is increasing, the demand of new fuel corresponds to a larger number of reactors than the ones from which the SNF can be recycled). As the increase in the fraction of burning technologies (SFR and ADS) is larger in the transition from the initial phase to the burning phase (2040–2060) than in the transition from the burning to the stabilization phases (2100–2120) as the bottom figure indicates, the reduction in

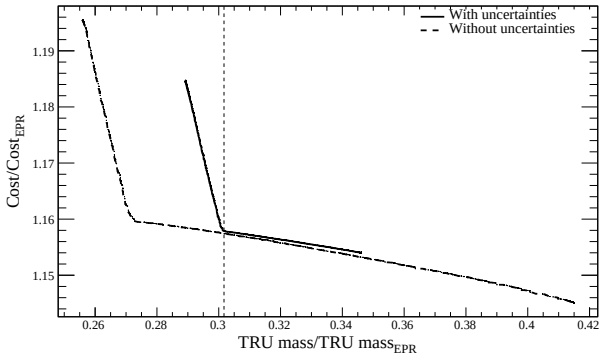

FIGURE 5 Comparison of the Pareto front with and without uncertainties.

Pu stock is more important during the first transition. Note that, as the Pu stock is completely exhausted at around year 2062, small perturbations may produce a lack of material breaking the scenario. Aside from this effect occurring at transitions, ~~for this case~~in this scenario, the Pu during the rest of the burning phase cannot be consumed (on the contrary, it is accumulated) due to a limitation in the burning technologies (ADS/SFR) that can be installed ~~in the fleet~~ to avoid a shortage of material. This can be observed again in the bottom graph noticing that the ADS and SFR energy share is higher during the last phase.

For the blue case neither ADS nor SFR reactors are deployed during the burning phase so the Pu inventories increase steadily during this phase. Hence, no scenario breaking can occur for this case although the stabilization of the inventories could be compromised in the presence of uncertainties. Obviously, as there are no burner reactors in the burning phase, the Pu inventories at the end of the scenario are much larger than for the previous case.

4.3 | Including the uncertainties

In this section the optimization problem is solved taking into account the uncertainties in the energy production and the reprocessing capacity, minimizing the expected values of the objectives functions approximated with Eq. (3) and averaging the penalty function too. The results will be compared with those obtained in Section 4.1 ~~to~~ not to establish a relation between both cases, but to identify the problems ~~derived~~ arising from not taking into account the uncertainties ~~in a first instance.~~ from the beginning.

The solutions are shown in Fig. 5 and Fig. 6. Fig. 5 compares the new Pareto front obtained with uncertainties (continuous line) with the Pareto front of Fig. 2 represented with the dashed line. The new Pareto front is located inside the region of non-dominant but feasible solutions obtained in the case without uncertainties (grey dots of Fig. 2). ~~Consequently, the~~ This is due to the fact that the case with uncertainties takes up a smaller region in the objective space than the case without uncertainties. This region that now is not accessible, corresponds to feasible solutions in the reference case for which the constraints cannot be fulfilled in the presence of uncertainties.

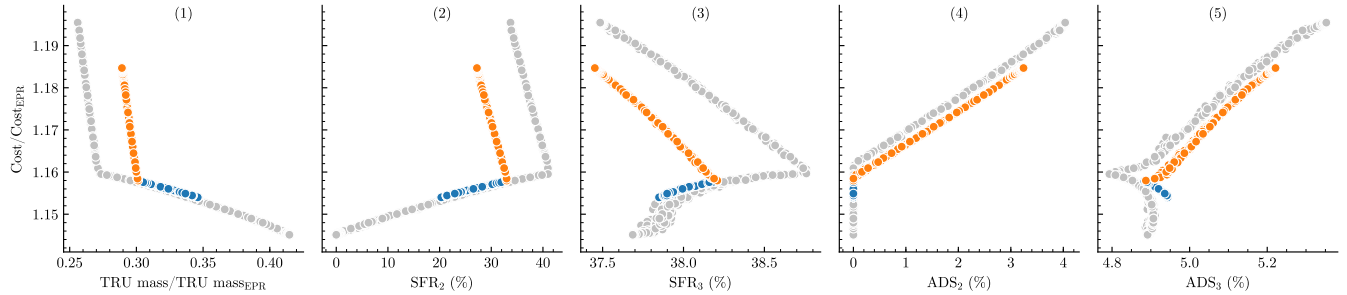

FIGURE 6 Scatter plots between cost and input parameters plus TRU inventories for the uncertainty case (in ~~color~~colour). In grey, the results of the reference case discussed in Sect. 4.1.

The solutions in the input parameter space are shown in Fig. 6 with the ~~colored~~ coloured points in blue and orange, and the grey dots being the results of the reference case (without uncertainties, last row in Fig. 3). For the shake of clarity, only the scatter plot between the cost and the other variables is represented; note that as in the previous case Fig. 5 corresponds to Fig. 6.1. Focusing on the blue and orange results, again two major clusters can be observed: Orange < 0.301 TRU mass/TRU mass$_{EPR}$ < Blue. Following the interpretation introduced in the previous section this can be identified again with TRU minimization (orange) and cost minimization (blue). For this particular case, the uncertainty solutions exhibit the same shape that was obtained in Section 4.1 but extending over a smaller region of the input parameter and objective spaces, so similar conclusions can be derived: the cost of the scenario increases linearly as the TRU mass is reduced until some point after which the trend changes sharply as a consequence of the introduction of ADS reactors. Finally, the blue solutions are almost coincident in the objective space with a region of the reference front, (although the case without uncertainties is always below), being the case with uncertainties a small region of the reference calculation. As the blue part of the Pareto front is very close to the reference one, the elbow of the L-shaped new front is located approximately at the frontier that was defined in the previous section, which divided the solutions based on the penalty violation (the vertical line is the same in both Fig. 5 and Fig. 2).

In general, the effect of the uncertainties is to shrink the solutions space: now the mass can only be reduced in a factor that ranges between 65%–71% with a cost increase of 16%–18.5%. From the comparison between the Pareto fronts, it can observed that for both the TRU and cost minimization, there are solutions that are now lost when compared to the reference case. As it was explained in the previous section, those solutions minimizing the TRU inventories violate the additional mass constraint in the presence of perturbations. Consequently, as the TRU reduction is limited when compared to the reference case, the maximum energy share of the ADS+SFR technologies during the burning phase must be lower when compared to that case, as the obtained results show when the ~~colored~~ coloured solutions are compared with the grey ones in Fig. 6.2 and Fig. 6.4. In the case of the lost solutions minimizing the costs, this effect is produced by the stabilization constraint. However, whereas the violation of the additional mass can be easily identified with an underlying physical effect (an excessive ADS+SFR energy share during the burning phase), for the stabilization condition no further explanation was found.

Finally, despite the fact that the results in both the reference and the uncertainty cases exhibit the same shape, some differences can be identified. Although in Figs. 6.2 to 6.4 the blue dots are very close to the dots of the reference calculation, in the case of the ADS share during the stabilization phase (Fig. 6.5) the solution lies in a region that is not accessible from the reference case. This agrees with the results of the previous section in which none of the reference solutions were found to be robust against perturbations. Moreover, it illustrates the problem of ignoring the uncertainties during the optimization process: by doing so, certain solutions that seems valid without uncertainties are not longer correct when they are considered. However, an important remark is the existence of an overlapping region between all input parameters but the installed power fraction of ADS during the stabilization phase. ~~This~~ The existence of this region indicates that the scenario can be corrected: if the reference input parameters were chosen in this zone, it would be possible to readapt the scenario in the presence of uncertainties towards an optimum sustainable state by changing the number of ADS during the stabilization phase. In this way, from a decision making point of view, there exist solutions more interesting than others given their ability of readaptation since if the input parameters were firstly chosen in these regions, it would be possible to correct the scenario before the stabilization phase occurs.

5 | CONCLUSIONS

The complexity of nuclear fuel cycle scenarios has driven in the recent years the development of automatic optimization tools that are able to obtain the best scenario or set of scenarios when precise objectives are pursued, a key task in decision making. Nonetheless, these analyses cannot be decoupled from the uncertainty ones since perturbations can break scenario equilibriums between facilities as several studies have shown. In this work, a methodology for optimizing electronuclear scenarios in the presence of uncertainties has been presented. To this end, the TR_EVOL fuel cycle code has been upgraded with the DEMO evolutionary multiobjective algorithm which was further extended for handling constraints and uncertainties. This methodology has been applied to an advanced and sustainable nuclear scenario consisting of EPR, ADS and SFR systems and ~~LWR~~ LWRs in the initial phase. The optimization problem aims to find the fleet shares of each technology that minimize both the TRU inventories and the cost after 300 years. Additionally, the energy production and the reprocessing capacity of the plants were assumed to be variables affected by uncertainty.

In a first approach, the two-objective optimization problem has been solved without considering uncertainties. It was found that it was not possible to minimize both objectives simultaneously. The Pareto front obtained indicates that the TRU inventories can be reduced by a factor that ranges between 60%–75% implying a cost increase of 15%–20% respectively when compared to an open fuel cycle strategy. However, a posterior analysis shows that these solutions were unstable, and thus the imposed scenario constraints will not be longer fulfilled in the presence of uncertainties. In this way, the uncertainties not only lead to a non-optimum solution but also compromise the robustness of the scenarios.

Secondly, the problem has been solved considering this time the effect of the uncertainties. Results have shown that their effect is to shrink the Pareto front when compared to the previous case as a consequence of constraint violation: the TRU reduction now ranges between 65%–71% while the cost between 16%–18.5%. Additionally, the ~~power~~ energy shares of the different technologies in the optimum solutions in the case with uncertainties are different than in the case without, although in some cases an overlapping region exists. Consequently, if these ~~input parameters~~ energy shares were firstly chosen in these regions, it would be possible to correct the scenario.

The obtained results evidence the fact that uncertainties play a major role in scenario optimization and must therefore be taken into account beforehand to ensure the reliability of the obtained solutions. Besides, the methodology presented can be implemented by any fuel cycle simulator able to perform a large number of simulations in a feasible amount of time. Although this approach is automatic, future works should focus on the massive data analysis required for identifying the physical process that constraints the solutions.

How to cite this article: A. V. Skarbeli, F. Álvarez-Velarde, and V. Bécares , (YEAR), TITLE, *Int. J. Energy Res.*, *VOLUME*.

APPENDIX

A INITIAL SNF LEGACY

The initial spent nuclear fuel legacy inventories of the scenario are provided in Table A1. The data has been extracted from [14], and has been disaggregated by year of inclusion and fuel type.

TABLE A1 Initial SNF stock per year of inclusion in the scenario and fuel type.

	UOX fuel (t)		MOX fuel (t)	
Year	2010	2022	2010	2022
^{234}U	5.40	0.25	0.20	0.15
^{235}U	207.50	78.50	2.00	2.70
^{236}U	148.50	40.20	0.40	0.50
^{238}U	27384.00	8247.30	1308.40	920.00
^{237}Np	19.10	5.70	0.30	0.30
^{238}Pu	8.00	2.00	2.30	1.00
^{239}Pu	170.90	49.30	29.90	19.20
^{240}Pu	75.20	21.00	20.40	14.60
^{241}Pu	39.30	6.70	9.80	3.00
^{242}Pu	23.30	5.50	7.50	4.50
^{241}Am	12.30	6.70	4.10	5.20
^{243}Am	5.90	1.40	2.00	0.90
^{242}Cm	0.20	0.00	0.00	0.00
^{244}Cm	1.80	0.40	0.90	0.20
^{245}Cm	0.10	0.04	0.10	0.06
Fission Products	1327.60	363.00	57.10	40.00
Total	29429.10	8827.99	1445.40	1012.31

ACRONYMS

ADS	Accelerator-Driven Subcritical System
CP-ESFR	Collaborative Project for a European Sodium Fast Reactor
DE	Differencial Evolution
DEMO	Differential Evolution for Multiobjective Optimization
EPR	European Pressurized Reactor
HM	Heavy Metal
LWR	Light Water Reactor
MA	Minor Actinides
MOX	Mixed Oxides
O&M	Operation & Maintenance
PWR	Pressurized Water Reactor
SFR	Sodium Fast Reactor
SNF	Spent Nuclear Fuel
TR_EVOL	Transition Evolution code
TRU	Transuranic
UOX	Uranium Oxide

ACKNOWLEDGEMENTS

This work was supported in part by the Spanish national company for radioactive waste management ENRESA, through the CIEMAT-ENRESA agreement on 'Transmutación de residuos radiactivos de alta actividad' and the Spanish 'Programa Estatal de I+D+i Orientada a los Retos de la Sociedad' project SYTRAD2 (ENE2017-89280-R).

References

1. OECD/NEA . *Transition Towards a Sustainable Nuclear Fuel Cycle*. No. 7133 in Nuclear ScienceOECD . 2013

2. IAEA . *Enhancing Benefits of Nuclear Energy Technology Innovation through Cooperation among Countries: Final Report of the INPRO Collaborative Project SYNERGIES*. No. NF-T-4.9 in Nuclear Energy SeriesVienna: International Atomic Energy Agency . 2018.

3. Freynet D, Coquelet-Pascal C, Eschbach R, Krivtchik G, Merle-Lucotte E. Multiobjective optimization for nuclear fleet evolution scenarios using COSI. *EPJ Nuclear Sciences & Technologies* 2016; 2: 9. doi: 10.1051/epjn/e2015-50066-7

4. Yue Q, He J, Zhi S, Dong H. Fuel cycles optimization of nuclear power industry in China. *Annals of Nuclear Energy* 2018; 111: 635–643. doi: 10.1016/j.anucene.2017.09.049

5. OECD/NEA . The Effects and of the Uncertainty of Input Parameters on Nuclear Fuel Cycle Scenario Studies. Nuclear Science NEA/NSC/R(2016)4: Paris. 2017.

6. Thiollière N, Clavel JB, Courtin F, et al. A methodology for performing sensitivity analysis in dynamic fuel cycle simulation studies applied to a PWR fleet simulated with the CLASS tool. *EPJ Nuclear Sciences & Technologies* 2018; 4: 13. doi: 10.1051/epjn/2018009

7. Skarbeli AV, Álvarez-Velarde F. Uncertainty quantification on advanced fuel cycle scenario simulations applying local and global methods. *Annals of Nuclear Energy* 2019; 124: 349–356. doi: 10.1016/j.anucene.2018.10.018

8. Kunsch PL, Teghem J. Nuclear fuel cycle optimization using multi-objective stochastic linear programming. *European Journal of Operational Research* 1987; 31(2): 240–249. doi: 10.1016/0377-2217(87)90028-2

9. Lee JW, Jeong Y, Chang YI, Chang SH. Linear programming optimization of nuclear energy strategy with sodium-cooled fast reactors. *Nuclear Engineering and Technology* 2011; 43. doi: 10.5516/NET.2011.43.4.383

10. Hays R, Turinsky P. Stochastic Optimization for Nuclear Facility Deployment Scenarios Using VISION. *Nuclear Technology* 2014; 186(1): 76–89. doi: 10.13182/nt13-68

11. Passerini S, Kazimi MS, Shwageraus E. A Systematic Approach to Nuclear Fuel Cycle Analysis and Optimization. *Nuclear Science and Engineering* 2014; 178(2): 186–201. doi: 10.13182/nse13-20

12. Álvarez-Velarde F, González-Romero EM. TR_EVOL, upgrading of EVOLCODE2 for transition scenario studies. In: OECD/NEA; 2010; Karlsruhe, Germany.

13. Merino-Rodríguez I, García-Martínez M, Álvarez-Velarde F, López D. Cross check of the new economic and mass balance features of the fuel cycle scenario code TR_EVOL. *EPJ Nuclear Sciences & Technologies* 2016; 2: 33. doi: 10.1051/epjn/2016029

14. Garzenne C, Bianchi F, Glinatsis G, et al. Scenarios of ESFR deployment in Europe. CP–ESFR SP2.1.1 D2 Contract Number 232658: 2011.

15. Rineiski A, Mériot C, Coquelet-Pascal C, Krepel J, Fridman E, Mikityuk K. Specification of the new core safety measures. ESFR-SMART D1.1.2.: 2018.

16. Artioli C, Glinatsis G, Petrovich C. EFIT Core Reference Cycle Analysis and Reactivity Coefficients. tech. rep., ENEA; Bologna: 2008.

17. Baker A, Ross R. Comparison of the value of plutonium and uranium isotopes in fast reactors. *USAEC, Breeding, Economics, and Safety in Large Fast Breeder Reactors (Argonne National Laboratory, Illinois, 1963)* 1963: 329–365.

18. Maeda S. Status of the Development of Fast Breeder Reactor Fuels in Fact Project. In: No. 1689 in TECDOC Series. Vienna: INTERNATIONAL ATOMIC ENERGY AGENCY. 2013 (pp. 19–24).

19. Rodríguez IM, Álvarez-Velarde F, Martín-Fuertes F. Analysis of advanced European nuclear fuel cycle scenarios including transmutation and economic estimates. *Annals of Nuclear Energy* 2014; 70: 240–247. doi: 10.1016/j.anucene.2014.03.015

20. Dixon BW, Ganda F, Williams KA, Hoffman E, Hanson JK. Advanced Fuel Cycle Cost Basis – 2017 Edition. tech. rep., 2017

21. Robič T, Filipič B. DEMO: Differential Evolution for Multiobjective Optimization. In: Springer Berlin Heidelberg. 2005 (pp. 520–533)

22. Storn R, Price K. Differential Evolution - A simple and efficient adaptive scheme for global optimization over continuous spaces. Tech. Rep. TR-95-012, International Computer Science Institute; Berlekey: 1995.

23. Storn R, Price K. Differential Evolution – A Simple and Efficient Heuristic for global Optimization over Continuous Spaces. *Journal of Global Optimization* 1997; 11(4): 341–359. doi: 10.1023/a:1008202821328

24. Takahama T, Sakai S. Constrained Optimization by ε Constrained Particle Swarm Optimizer with ε-level Control. In: Springer Berlin Heidelberg. 2005 (pp. 1019–1029)

25. Hannah LA. Stochastic Optimization. In: Elsevier. 2015 (pp. 473–481)